Figure 4 *(see previous page)*
Effect of depletion and over expression of Hsc70 in TG cells on bacterial internalization. (A) Depletion of Hsc70. TG cells were treated for 48 h with siRNA targeting Hsc70 or without it (reagent only or no treatment), or β-actin or the control (QIAGEN AllStars Negative Control). Expression of the indicated proteins was monitored by immunoblotting. β-actin was used as an internal control. (B) Over expression of Hsc70. TG cells were transfected with or without (control) pcDNA4/TO-Hsc70 or vector only. (C) Bacterial internalization into Hsc70 depleted (siRNA) or over expressed (over exp.) TG cells was studied in a bacterial internalization assay. Lanes correspond to panels A and B. Data are the averages of triplicate samples from three identical experiments, and the error bars represent the standard deviations. Statistically significant differences between bacterial internalization into TG cells with (Hsc70) and without siRNA (control), and over expression and the control (vector) are indicated by asterisks (*, $P < 0.01$). (D) Distribution of Hsc70 in non-treated (control), Hsc70 depleted (siRNA), or over expressed (over expression) TG cells. Fluorescence microscopy of stained TG cells with the R2–25 antibody (upper panels) and phase contrast microscopy of the corresponding microscopic fields (lower panels) are shown.

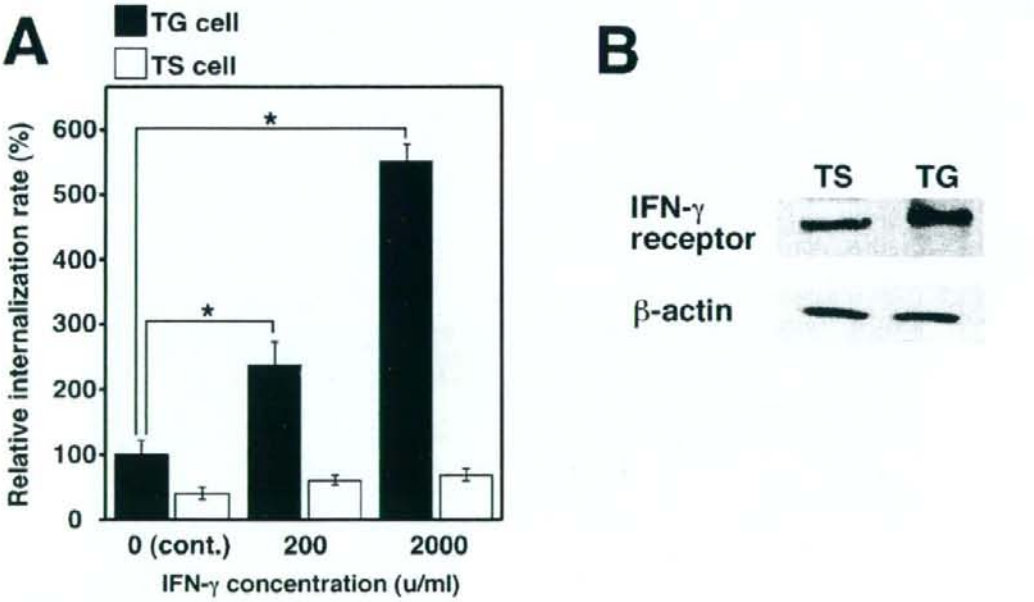

Figure 5
IFN-γ promotes bacterial internalization into TG cells. (A) Bacterial internalization into IFN-γ treated TS or TG cells. *B. abortus* was deposited onto TS and TG cells which were treated with or without (cont.) IFN-γ at the indicated concentrations. Data are the averages of triplicate samples from three identical experiments, and the error bars represent the standard deviations. Statistically significant differences between bacterial internalization in TG cells with and without IFN-γ treatment are indicated by asterisks (*, $P < 0.01$). (B) Expression of IFN-γ receptor in TS and TG cells. Immunoblot analysis was performed with anti-IFN-γ receptor and anti-β-actin rabbit polyclonal antibody.

by transfecting the Hsc70 expression vector into TG cells. After 48 h, expression levels of Hsc70 were significantly higher than the control levels (Fig. 4B and 4D). The internalization efficiency of *B. abortus* into TG cells in which Hsc70 was over-expressed was significantly higher than the control levels (Fig. 4C).

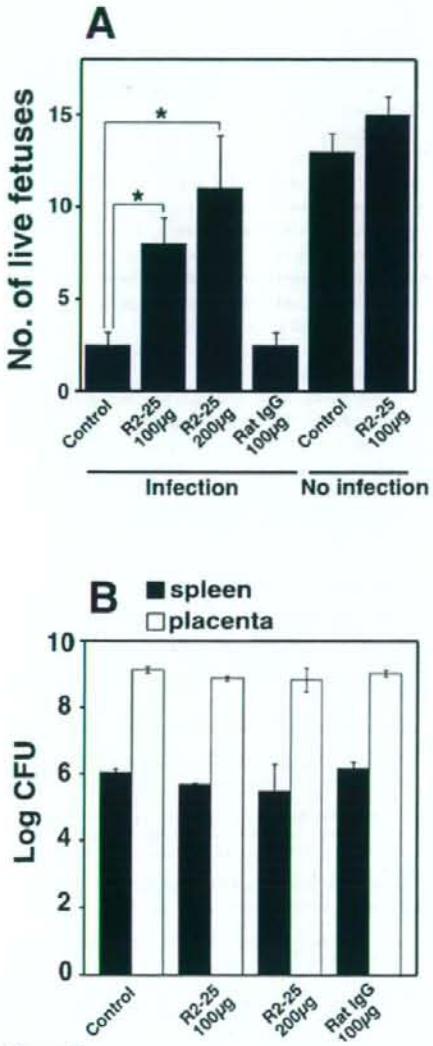

Figure 6

Preventing abortion by inoculating with anti-Hsc70 antibody. (A) Number of live fetuses. Hsc70 was neutralized in the mice by administering with or without (control) an anti-mouse Hsc70 monoclonal antibody (clone R2–25)*in vivo* using 100 or 200 μg of the antibody. The control mice were given 100 μg of normal rat IgG. Statistically significant differences between the untreated control and antibody treated mice are indicated by asterisks (*, $P < 0.01$). (B) Bacterial numbers in spleen and placenta. On day 18.5 of gestation, the placenta and spleen were removed and homogenized in PBS. Tissue homogenates were serially diluted with PBS and plated on Brucella agar in order to count the number of CFU in each organ.

IFN-γ enhances bacterial uptake by TG cells

Since a transient increase in IFN-γ brought about by *Brucella* infection promotes abortion in pregnant mice [10], we investigated the effect of IFN-γ treatment on bacterial internalization and Hsc70 expression in TG cells. IFN-γ treatment significantly increased the internalization efficiency of *B. abortus* into TG cells as their concentration, but had no effect in TS cells (Fig. 5A). To determine whether the enhancement of bacterial internalization by IFN-γ treatment was due to up-regulate Hsc70 expression or not, RNA was isolated from IFN-γ treated TG cells and subjected to RT-PCR. This showed that IFN-γ treatment did not affect Hsc70 expression (data not shown). IFN-γ receptor was expressed in TS and TG cells (Fig. 5B).

Preventing abortion by inoculating pregnant mice with anti-Hsc70 antibody

To determine if abortion is prevented by neutralizing the Hsc70 expressed on TG cells in the mouse placenta, pregnant mice were inoculated with the R2–25 antibody 24 h before infection with *B. abortus*, which was done on day 4.5 of gestation. While there was no change in the number of abortions observed in the non-inoculated mice, there was a significant increase in number of live fetuses in the inoculated mice (Fig. 6A). Inoculation of uninfected pregnant mice with the R2–25 antibody did not affect on pregnancy (Fig. 6A). Upon examining bacterial numbers in the spleen and placenta of infected pregnant mice, it was found that bacterial numbers were similar in both mice inoculated with the R2–25 antibody and those not inoculated with it (Fig. 6B).

Discussion

Previous mouse model studies have shown that *Brucella abortus* specifically replicates in trophoblast giant (TG) cells in the placenta [9,10]. TG cells are polyploid cells that play a crucial role in implantation, in remodeling of the embryonic cavity, and preventing maternal blood

flow to the implantation site [22]. Since *B. abortus* internalizes into TG cells and replicates in them, cell functions are not exhibited completely, which leads to abortion since implantation and placental development are inhibited. Therefore, it is thought that bacterial infection of TG cells is a key event in inducing abortion. To analyze the molecular mechanisms of *B. abortus* infection of TG cells *in vitro*, we used trophoblast stem (TS) cells and TG cells differentiated from TS cells for the infection assay in this study. Although TG cell differentiation is fairly well understood at the morphological and molecular level [23], the role of immune responses in fighting against pathogens of TG cells is poorly understood and in this regard a model of host-pathogen interaction using TG cells would be useful for obtaining new information of the effect of TG cell functions on pregnancy.

Hsc70 has been reported to be present on the surface of several types of cells [24]. In this regard, though Hsc70 congregates on the surface of TG cells, it is present to a much lesser extent on the surface of TS cells (data not shown). This may be a reason that the internalization of *B. abortus* into TG cells was greater than that into TS cells. As Hsc70 and many other factors will be present on TG cells differentiated from TS cells, there is a possibility that other receptors or bacterial uptake-associated molecules may contribute to *B. abortus* infection of TG cells. Little is known about how Hsc70, a protein with no signal sequence for secretion, exits cells by mechanisms other than escape from cells undergoing necrotic lysis. In previous studies, Hsc70 has seen to be released from a late endsomal lysosomal location where it participates in protein degradation [25,26]. Further, the secretion of the Hsp70 family and its association with lipid rafts have also been observed in epithelial cells under normal conditions, and a lipid raft-based mechanism has been suggested for the membrane delivery and release of Hsp70 family [27]. Although receptors for the extracellular Hsp70 family have still not been fully defined, several cell surface receptors have been suggested, such as CD14, CD40, CD91 and scavenger receptor Lox-1 [28-31]. Since it has also been noted that class A scavenger receptor (SR-A) contributes to *B. abortus* infection in macrophages [32], SR-A may be receptors for Hsc70, and the mechanism for *B. abortus* internalization into TG cells may be the same pathway as that for Hsc70 uptake by TG cells. Hsc70 may have a function that is catching antigens and anti-Hsc70 would inhibit binding between Hsc70 and antigens. IFN-γ treatment enhanced bacterial internalization into TG cells and these observations agreed with results obtained in pregnant mice model [10], and thus expression of unidentified receptors against Hsc70 may be upregulated by IFN-γ treatment. IFN-γ should therefore promote internalization of *B. abortus* into TG cells *in vivo* and this would be one of ways in which infectious abortion is induced.

Conclusion

The finding of this study that the anti-Hsc70 antibody prevents abortion caused by *B. abortus* infection is expected to be applied in the development of methods of preventing abortion. Since intracellular bacteria such as *Brucella* replicate in host cells, it is difficult to completely eliminate them from the host through treatment with antibiotics and develop effective vaccines against them. An alternative strategy in treating infection due to *Brucella* would be inhibition of bacterial internalization into TG cells and this could be an effective means of protecting against abortion due to brucellosis. Recently, Carvalho Neta *et al.* reported that *B. abortus* modulates innate immune response by bovine trophoblastic cells [33]. Although the structure of bovine placenta is completely different from mouse placenta, bovine and mouse trophoblastic cells may have similar function in the immune system. However, it is not known whether the mechanism of host-pathogen interaction observed in this study could be used to develop protective methods against other abortion-inducing pathogen infections, and thus further analysis of TG cell function in the immune system will be needed to clarify host defense mechanisms in the placenta and those contributing to the success of pregnancy.

Authors' contributions

MW conceived the study. MW, HS and KW designed the experiments, interpreted the results and worked on the manuscript. KW and MT carried out most of the experimental work. ST, HF and MH participated in cell culture and pathological experiments. HS and MW participated in animal experiments. All authors read and approved the final manuscript.

Acknowledgements

We thank Dr. Alexander Cox for critical reading of the manuscript, and Dr. Suk Kim for valuable discussion. This work was supported, in part, by grants from Program for Promotion of Basic Research Activities for Innovative Biosciences (PROBRAIN), and grants from the Naito Fundation, and Institute for Fermentation, Osaka.

References

1. Givens MD: **A clinical, evidence-based approach to infectious causes of infertility in beef cattle.** *Theriogenology* 2006, **66**:648-54.
2. Ko J, Splitter GA: **Molecular host-pathogen interaction in brucellosis: current understanding and future approaches to vaccine development for mice and humans.** *Clin Microbiol Rev* 2003, **16**:65-78.
3. Pappas G, Papadimitriou P, Akritidis N, Christou L, Tsianos EV: **The new global map of human brucellosis.** *Lancet Infect Dis* 2006, **6**:91-99.
4. Khan MY, Mah MW, Memish ZA: **Brucellosis in pregnant women.** *Clin Infect Dis* 2001, **32**:1172-1177.
5. Samartino LE, Enright FM: **Pathogenesis of abortion of bovine brucellosis.** *Comp Immunol Microbiol Infect Dis* 1993, **16**:95-101.
6. Anderson TD, Cheville NF, Meador VP: **Pathogenesis of placentitis in the goat inoculated with *Brucella abortus*. II. Ultrastructural studies.** *Vet Pathol* 1986, **23**:227-239.
7. Meador VP, Deyoe BL: **Intracellular localization of *Brucella abortus* in bovine placenta.** *Vet Pathol* 1989, **26**:513-515.

8. Anderson TD, Meador VP, Cheville NF: **Pathogenesis of placentitis in the goat inoculated with *Brucella abortus*. I. Gross and histologic lesions.** *Vet Pathol* 1986, **23**:219-226.
9. Tobias L, Cordes DO, Schurig GG: **Placental pathology of the pregnant mouse inoculated with *Brucella abortus* strain 2308.** *Vet Pathol* 1993, **30**:119-129.
10. Kim S, Lee DS, Watanabe K, Furuoka H, Suzuki H, Watarai M: **Interferon-γ promotes abortion due to *Brucella* infection in pregnant mice.** *BMC Microbiol* 2005, **5**:22.
11. Raghupathy R: **Th1-type immunity is incompatible with successful pregnancy.** *Immunol Today* 1997, **18**:478-482.
12. Wegmann TG, Lin H, Guilbert L, Mosmann TR: **Bidirectional cytokine interactions in the maternal-fetal relationship: is successful pregnancy a Th2 phenomenon?** *Immunol Today* 1993, **14**:353-356.
13. Weinberg ED: **Pregnancy-associated immune suppression: risks and mechanisms.** *Microb Pathog* 1987, **3**:393-397.
14. Krishnan L, Guilbert LJ, Russell AS, Wegmann TG, Mosmann TR, Belosevic M: **Pregnancy impairs resistance of C57BL/6 mice to *Leishmania major* infection and causes decreased antigen-specific IFN-gamma response and increased production of T helper 2 cytokines.** *J Immunol* 1996, **156**:644-652.
15. Sano M, Mitsuyama M, Watanabe Y, Nomoto K: **Impairment of T cell-mediated immunity to *Listeria monocytogenes* in pregnant mice.** *Microbiol Immunol* 1986, **30**:165-176.
16. Watarai M, Makino S, Shirahata T: **An essential virulence protein of *Brucella abortus*, VirB4, requires an intact nucleoside-triphosphate-binding domain.** *Microbiology* 2002, **148**:1439-1446.
17. Watarai M, Makino S, Fujii Y, Okamoto K, Shirahata T: **Modulation of *Brucella*-induced macropinocytosis by lipid rafts mediates intracellular replication.** *Cell Microbiol* 2002, **4**:341-355.
18. Tanaka S, Kunath T, Hadjantonakis AK, Nagy A, Rossant J: **Promotion of trophoblast stem cell proliferation by FGF4.** *Science* 1998, **282**:2072-2075.
19. Kim S, Watarai M, Kondo Y, Erdenebaatar J, Makino S, Shirahata T: **Isolation and characterization of mini-Tn*5*Km2 insertion mutants of *Brucella abortus* deficient in internalization and intracellular growth in HeLa cells.** *Infect Immun* 2003, **71**:3020-3027.
20. Pizarro-Cerda J, Cossart P: **Bacterial adhesion and entry into host cells.** *Cell* 2006, **124**:715-727.
21. Parast MM, Aeder S, Sutherland AE: **Trophoblast giant-cell differentiation involves changes in cytoskeleton and cell motility.** *Dev Biol* 2001, **230**:43-60.
22. Cross JC: **Genetic insights into trophoblast differentiation and placental morphogenesis.** *Semin Cell Dev Biol* 2000, **11**:105-113.
23. Cross JC: **How to make a placenta: mechanisms of trophoblast cell differentiation in mice-a review.** *Placenta* 2005, **26(Suppl A)**:S3-9.
24. Multhoff G, Hightower LE: **Cell surface expression of heat shock proteins and the immune response.** *Cell Stress Chaperones* 1996, **1**:167-176.
25. Isenman LD, Dice JF: **Secretion of intact proteins and peptide fragments by lysosomal pathways of protein degradation.** *J Biol Chem* 1989, **264**:21591-621596.
26. Terlecky SR, Olson TS, Dice JF: **A pathway of lysosomal proteolysis mediated by the 73-kilodalton heat shock cognate protein.** *Acta Biol Hung* 1991, **42**:39-47.
27. Broquet AH, Thomas G, Masliah J, Trugnan G, Bachelet M: **Expression of the molecular chaperone Hsp70 in detergent-resistant microdomains correlates with its membrane delivery and release.** *J Biol Chem* 2003, **278**:21601-21606.
28. Asea A, Kraeft SK, Kurt-Jones EA, Stevenson MA, Chen LB, Finberg RW, Koo GC, Calderwood SK: **HSP70 stimulates cytokine production through a CD14-dependant pathway, demonstrating its dual role as a chaperone and cytokine.** *Nat Med* 2000, **6**:435-442.
29. Becker T, Hartl FU, Wieland F: **CD40, an extracellular receptor for binding and uptake of Hsp70-peptide complexes.** *J Cell Biol* 2002, **158**:1277-1285.
30. Delneste Y, Magistrelli G, Gauchat J, Haeuw J, Aubry J, Nakamura K, Kawakami-Honda N, Goetsch L, Sawamura T, Bonnefoy J, Jeannin P: **Involvement of LOX-1 in dendritic cell-mediated antigen cross-presentation.** *Immunity* 2002, **17**:353-362.
31. Srivastava P: **Interaction of heat shock proteins with peptides and antigen presenting cells: chaperoning of the innate and adaptive immune responses.** *Annu Rev Immunol* 2002, **20**:395-425.
32. Kim S, Watarai M, Suzuki H, Makino S, Kodama T, Shirahata T: **Lipid raft microdomains mediate class A scavenger receptor-dependent infection of *Brucella abortus*.** *Microb Pathog* 2004, **37**:11-19.
33. Carvalho Neta AV, Stynen AP, Paixão TA, Miranda KL, Silva FL, Roux CM, Tsolis RM, Everts RE, Lewin HA, Adams LG, Carvalho AF, Lage AP, Santos RL: **Modulation of the bovine trophoblastic innate immune response by *Brucella abortus*.** *Infect Immun* 2008, **76**:1897-907.

JVI Accepts, published online ahead of print on 28 January 2009
J. Virol. doi:10.1128/JVI.01740-08

The region approximately between amino acids 81 and 137 of proteinase K-resistant PrP^{Sc} is critical for the infectivity of the Chandler prion strain

Running title: Infectivity of N-terminal truncated PrP^{Sc}

Ryo Shindoh, Chan-Lan Kim[†], Chang-Hyun Song, Rie Hasebe, and Motohiro Horiuchi*

Laboratory of Prion Diseases, Graduate School of Veterinary Medicine, Hokkaido University, Kita 18, Nishi 9, Kita-ku, Sapporo 060-0818, Japan

[†]Present address: Foreign Animal Disease Division, Animal Disease Control Department, National Veterinary Research and Quarantine Service, 480 Anyang-6 dong, Manan-gu, Anyang 430-824, Republic of Korea

*Correspondence to (and present address): Motohiro Horiuchi, DVM, Ph.D.
Laboratory of Prion Diseases,
Graduate School of Veterinary Medicine,
Hokkaido University,
Kita 18, Nishi 9, Kita-ku,
Sapporo 060-0818, Japan
Phone/Fax: +81-11-706-5293
e-mail:horiuchi@vetmed.hokudai.ac.jp

Word count: Abstract, 249; Text; 4,344.

Abstract

Although the major component of prion is believed to be the oligomer of PrP^{Sc}, little information is available concerning regions on the PrP^{Sc} molecule that affect prion infectivity. During the analysis of PrP^{Sc} from various prion strains, we found that PrP^{Sc} of the Chandler strain showed a unique property in the conformational-stability assay, and this property appeared useful for studying the relation between regions of the PrP^{Sc} molecule and prion infectivity. Thus, we analyzed PrP^{Sc} of the Chandler strain in detail and analyzed infectivities of the N-terminally denatured and truncated proteinase K-resistant PrP. The N-terminal region of PrP^{Sc} of the Chandler strain showed a region-dependent resistance to guanidine hydrochloride (GdnHCl) treatment. The region approximately between amino acids (aa) 81 and 137 began to be denatured by the treatment with 1.5 M GdnHCl. Within this region, the region comprised of approximately aa 81-90 was denatured almost completely with 2 M GdnHCl. Furthermore, the region approximately between aa 90 and 137 was denatured completely with 3 M GdnHCl. However, the C-terminal region thereafter was extremely resistant to the GdnHCl treatment. This property was not observed in PrP^{Sc} of other prion strains. Denaturation of the aa 81-137 region by 3 M GdnHCl significantly prolonged the incubation periods compared to the untreated control. More strikingly, denaturation and removal of this region nearly abolished the infectivity. This suggests that the conformation of the region between aa 81 and 137 of the PrP^{Sc} molecule of the Chandler strain is directly associated with the prion infectivity.

INTRODUCTION

Prion diseases, such as scrapie, bovine spongiform encephalopathy (BSE) and Creutzfeldt-Jakob disease, are fatal neurodegenerative disorders characterized by accumulation of a disease-specific, abnormal isoform of the prion protein (PrP^{Sc}) in the central nervous system, astrogliosis, neuronal vacuolation and neuronal cell death. PrP^{Sc} is believed to generate from a cellular form of prion protein (PrP^{C}) by a post-translational modification including conformational transformation. Although the entity of prion, the causative agent of prion diseases, remains to be elucidated, PrP^{Sc} is believed to be a major component of the prion.

Direct interaction between PrP^{C} and pre-existing PrP^{Sc} precedes the transformation of PrP^{C} into newly generated PrP^{Sc}. Data on the regions of PrP^{C} that are indispensable for the PrP^{Sc} formation and prion propagation have been accumulated using neuroblastoma cells persistently infected with prion and transgenic mice expressing mutant PrPs. Although the extreme N-terminal region from amino acid (aa) 23 to 32 modulates prion propagation (8, 9, 34), the region between aa 32 and around 90 is not essential for production of PrP^{Sc} and propagation of the prion (9, 18, 22, 39). The residues 114-121, the most amyloidgenic region of PrP, is essential for conversion of PrP^{C} into PrP^{Sc} (14, 23). A deletion mutant lacking the residues 23-88 and 141-176 can convert into PrP^{Sc} and support prion propagation in transgenic (Tg) mice, suggesting that the residues 141-176 is not essential for prion propagation (22, 34). The cysteine residue at 178 that forms an intramolecular disulfide bond with another cysteine residue at 213 is essential for PrP^{Sc} formation (22). Additionally, amino acid substitutions at 167 and 218 prevent the PrP^{Sc} formation and showed dominant-negative effect on prion propagation (15, 28). On the contrary, due to the difficulty of direct manipulation of PrP^{Sc}, the regions of PrP^{Sc} that are important for the prion

infectivity have not been elucidated. It is well accepted that not the removal of the protease-sensitive N-terminal domain (aa 23 to around 90) from PrP^{Sc} but the denaturation of the remaining C-terminal domain diminishes the prion infectivity. However, the relationship between prion infectivity and the region(s) of PrP^{Sc} is largely unclear.

From the analysis of biochemical properties of PrP^{Sc} of various prion strains, we found that PrP^{Sc} of the Chandler strain has a region-dependent resistance to denaturation by guanidine hydrochloride (GdnHCl). This property allows for the denaturation and removal of specific regions of PrP^{Sc}. In this study, we describe the unique conformational stability of PrP^{Sc} of the Chandler strain and the region approximately between aa 81 and 137 of PrP^{Sc} is important for the infectivity of the Chandler prion strain.

MATERIALS AND METHODS

Mice and prion strains. Mouse-adapted prion strains 22L (7), Chandler (17), Fukuoka-1 (35), G1 (unpublished), and Obihiro (32) were used in this study. These mouse-adapted strains were propagated in female Jcl:ICR mice (CLEA Japan) except where otherwise specified. In some cases, C56BL/6J (CLEA Japan), RIII/J and I/LnJ mice (Jackson Laboratories) were used for prion propagation. In addition, BSE-derived mouse-adapted prion strains, designated KUS-m and TE-m, which were obtained by a third serial passage of Japanese BSE cases KUS and TE with RIII/J and C57BL/6J mice, respectively, were also used. All procedures for animal experiments were carried out according to protocols approved by the Institutional Committee for Animal Experiments.

Antibodies. Anti-PrP mAbs 110, 118, 147, 31C6, 43C5 and 44B1 (16) were used. In

addition, B103 rabbit polyclonal antibodies (pAb) raised against bovine PrP synthetic peptide aa 103-121 that corresponds to the aa 90-109 of mouse PrP were also used (12).

Conformational-stability assay. Conformational-stability assays were carried out as described by Legname et al. (19, 20) with some modifications. Brains of mice infected with prion were homogenized in phosphate-buffered saline (PBS) to make 10% homogenates. Aliquots of the homogenates were stored at –30 °C until use. The 10% brain homogenates (50 µl) were mixed with equal volumes of various concentrations of GdnHCl (0 to 8 M) and incubated with 37 °C for 1 h. Samples were then diluted by adding 850 µl of NTS buffer (10 mM Tris-HCl [pH 8.0], 150 mM NaCl, 0.5% Triton X-100 and 0.5% sodium deoxycholate). To adjust the final GdnHCl concentration to 0.4 M, 50 µl of various concentrations of GdnHCl (0 to 8 M) was added to each sample. The samples were then digested with proteinase K (PK; Roche) at 20 µg/ml for 30 min at 37 °C. After terminating PK activity by adding Pefabloc (Roche) to a final concentration at 2 mM, 500 µl of a 5:1 mixture of 2-butanol and methanol was added, mixed well, and kept for 10 min at ambient temperature. PrP^{Sc} was pelleted by centrifugation at 20,000 x g for 10 min at 20 °C. The resulting pellet was dissolved in 1x SDS sample buffer (62.5 mM Tris-HCl [pH 6.8], 5% glycerol, 3 mM EDTA, 4% β-mercaptoethanol, 0.04% bromophenol blue, 5% SDS, 4 M Urea) by boiling for 5 min. SDS-PAGE and immunoblotting were carried out as described elsewhere (38). The chemiluminescence intensities of bands of PrP^{Sc} were measured with a LAS-3000 chemiluminescence image analyzer (Fujifilm). Quantitative analyses of the blots were carried out with Image Reader LAS-3000 version 1.11 (Fujifilm). The sigmoidal patterns of denaturation curves were plotted using a non-linear least-squares fit. The concentrations of GdnHCl required to denature 50% of PrP^{Sc} ($[GdnHCl]_{1/2}$) were estimated from the denaturation curves and statistical analysis was carried out with one-way ANOVA followed

120 by a Newmann-Kuels test.

121

122 **Deglycosylation.** The 10% of brain homogenates (250 µl) were mixed with equal
123 volumes of the NTS buffer and digested with PK at 20 µg/ml for 1 h at 37 °C. Proteolysis
124 was terminated by addition of Pefabloc to a finial concentration at 4 mM. Samples were
125 then mixed with 1/5 volume of 5x denaturation buffer (20 mM Tris-HCl [pH 7.5], 150 mM
126 NaCl, 2 mM EDTA, 5% SDS, 10% β-mercaptoethanol) and 5 units of N-Glycosidase F
127 (Roche), and incubated for 16 h at 37 °C. Proteins were precipitated by adding 1/2 volume
128 of a 5:1 mixture of 2-butanol and methanol followed by centrifugation at 20,000 x g for 10
129 min at 20 °C.

130

131 **Preparation of cell lysates.** Neuro2a subclone persistently infected with the Chandler
132 strain (ScN2a-5; 38) was used. ScN2a-5 cells grwon in 10-cm dishes were collected by cell
133 scraper and pelleted by centrifugation at 300 x g for 5 min. The cells were washed once
134 with PBS and pelleted again by centrifugation. Resulting pellets were lysed with 1 ml of
135 lysis buffer (10 mM Tris-HCl [pH 7.5], 0.5% Triton X-100, 0.5% sodium deoxycholate, 150
136 mM NaCl, 5 mM EDTA) for 30 min on ice. Nuclei and cell debris were removed by low
137 speed centrifugation at 300 x g, supernatants were further centrifuged at 100,000 x g for 30
138 min at 4 °C. The resulting pellets were suspended with 50 µl PBS and used for
139 conformational-stability assays as the PrP^{Sc}-enriched fraction.

140

141 **Bioassay.** The 10% brain homogenates (540 µl) were mixed with equal volumes of
142 various concentrations of GdnHCl solution (0 to 6 M) and then incubated at 37 °C for 1 h.
143 Samples were then diluted by addition of 9.18 ml of NTS buffer and 540 µl of various
144 concentrations of GdnHCl solution was added to adjust the final concentration of GdnHCl to

0.4 M. The mixtures were ultracentrifuged at 197,000 x g for 2.5 h at 4 °C, and the resulting pellet was resuspended with 540 µl of PBS and used for the bioassay. The small aliquots of the samples were digested with PK and analyzed by immunoblotting to confirm the existence of PrP^{Sc}. To prepare the PK-treated inoculums for the bioassay, 540 µl of 10% brain homogenates were treated with GdnHCl as described above. After the GdnCHl treatment, samples were digested with 10 µg/ml of PK for 1 h at 37 °C, and digestion was stopped by adding Pefabloc to a final concentration of 2 mM. Samples were ultracentrifuged and the resulting pellets were resuspended with PBS as described above. Samples (20 µl) were intracerebrally inoculated into 4-week-old female Jcl:ICR mice.

RESULTS

Conformational stability of PrP^{Sc} of the mouse-adapted prion strains. To examine biochemical differences of PrP^{Sc} from various mouse-adapted prion strains, the conformational-stability assays were carried out to assess the resistance of PrP^{Sc} to denaturation by GdnHCl (Fig. 1A). When immunoblots were probed with pAb B103 and mAb 44B1 that recognize aa 90-109 and aa 155-231 of mouse PrP, respectively, the amount of PrP^{Sc} of the G1, Obihiro and Fukuoka-1 strains were nearly unchanged up to 2M GdnHCl treatment. The treatment with 2.5 M GdnHCl led to the first decrease in the amount of PrP^{Sc}, and only a trace amount of PrP^{Sc} was detected after the treatment with 3 M GdnHCl. The concentration of GdnHCl required to denature 50% of PrP^{Sc} ($[GdnHCl]_{1/2}$) was estimated from the denaturation curve of each prion strain (Fig. 1A). The $[GdnHCl]_{1/2}$ of the G1, Obihiro and Fukuoka-1 strains from the results of mAb 44B1 ranged from 2.0 to 2.1 M and there was no significant difference among them (Table 1). This indicates that these strains

have similar resistance to GdnHCl treatment. In contrast, $[GdnHCl]_{1/2}$ of the 22L strain was significantly lower than those of the G1, Obihiro and Fukuoka-1 strains, indicating that PrP^{Sc} of the 22L strains is less stable than that of other strains. Moreover, the $[GdnHCl]_{1/2}$ of BSE-derived strains, KUS-m and TE-m, were higher than other mouse-adapted prion strains except for the Chandler strain. The incubation periods of each prion strain and the $[GdnHCl]_{1/2}$ values are summarized in Table 1. Although the $[GdnHCl]_{1/2}$ values are comparable among the G1,Obihiro and Fukuoka strains, the G1 strain had an extremely long incubation periods.

Among the prion strains used in this study, PrP^{Sc} of the Chandler strain showed a unique alteration in molecular weight with the increase of GdnHCl concentration. When the blots were probed with pAb B103, approximately 1-2 kDa smaller PrP^{Sc} bands were detected with the 2.0 and 2.5 M GdnHCl treatments, and PrP^{Sc} was almost undetectable with the 3 M GdnHCl treatment. When the blots were probed with mAb 44B1, approximately 6-7 kDa smaller PrP^{Sc} bands were detected by the treatment with more than 2.0 M GdnHCl, and those were still detected even after the treatment with 3.5 M GdnHCl. The $[GdnHCl]_{1/2}$ of PrP^{Sc} of the Chandler strain was estimated as 3.2 M from the results of mAb 44B1.

Further characterization of the GdnHCl resistance of PrP^{Sc} of the Chandler strain. The results of the conformational-stability assays suggested that the N- and C-terminal regions of PK-resistant PrP^{Sc} of the Chandler strain have different resistance to GdnHCl treatment. Thus, we analyzed PrP^{Sc} of the Chandler strain more precisely with six additional mAbs (Fig. 2). Using mAb 110 recognizing repetitive amino acid sequences at 59-65 and 83-89, PrP^{Sc} was undetected with treatments of more than 2 M GdnHCl. The major N-terminus of PK-resistant core of PrP^{Sc} (called as PrP27-30) of the ME7 and Obihiro strains is reported to be a Gly at aa 81 (10, 11). Moreover, the molecular weight of de-glycosylated

Chandler PrP^{Sc} is identical to that of the Obihiro strain (Fig. 1B). Taken together, the major N-terminus of PK-resistant core of the Chandler PrP^{Sc} is expected to be at aa 81. We assumed therefore that the 1-2 kDa smaller PrP^{Sc} bands detected with pAb B103 with 2.0 and 2.5 M GdnHCl treatments resulted from the denaturation and removal of the region between aa 81 and around 90 (hereafter referred to as aa 90) of mouse PrP^{Sc}. The PrP^{Sc} patterns detected by mAb 132 appeared to be almost identical to those detected by pAb B103, indicating the region between aa 90 and the epitope for mAb 132 (aa 119-127) were almost denatured with treatment of more than 3 M GdnHCl. With more than 2 M GdnHCl treatments, the presence of the approximately 6-7 kDa smaller PrP^{Sc} bands was evident on the blots using mAb 31C6 (recognizing aa 143-149) and mAbs recognizing the C-terminal region thereafter (mAbs 43C5, 44B1, and 147). With 2.0 and 2.5 M GdnHCl treatments, the 6-7 kDa smaller PrP^{Sc} bands are thought to overlap with the 1-2 kDa smaller PrP^{Sc} bands that were detected with pAb B103 and mAb 132. Therefore, the presence of the 6-7 kDa smaller PrP^{Sc} was more obvious with treatment of more than 3 M GdnHCl, at which the N-terminal region of PK-resistant core of PrP^{Sc} between aa 81 and the epitope for mAb 132 was denatured and undetectable after PK digestion. The mAb 118 that recognizes aa 137-143 of mouse PrP also reacted with the 6-7 kDa smaller PrP^{Sc} bands (Fig. 2). This suggests that the truncated PK-resistant PrP^{Sc} lacks the N-terminal region up to around aa 127-137, although the exact N-terminus remains to be determined (hereafter referred to as aa 137). Taken together, these results indicate that PK-resistant core of PrP^{Sc} (aa 81-231) of the Chandler strain has a region-dependent conformational stability to GdnHCl treatment. The aa 81-90 of PrP^{Sc} is the most sensitive to GdnHCl and denatured almost completely with 2 M GdnHCl. Secondly, the region between aa 90 and 137 is denatured almost completely by more than 3 M GdnHCl, while the remaining C-terminal region of PrP^{Sc} is highly resistant to GdnHCl. The N-terminally truncated non-glycosylated PrP^{Sc} was detectable with 1.5 M GdnHCl treatment

220 (Fig. 2, arrowheads in mAbs 31C6, 43C5, 44B1, and 147), suggesting that the region between
221 aa 81 and 137 begins to be denatured with 1.5 M GdnHCl treatment. In contrast to the
222 Chandler strain, PrP^{Sc} of the Obihiro strain was nearly undetected with 3 M GdnHCl
223 treatment independent of antibodies and the $[GdnHCl]_{1/2}$ values estimated from each blot
224 were comparable (Fig. 2).

225 The 6-7 kDa smaller unglycosylated PrP^{Sc} was occasionally detected by mAbs
226 recognizing the C-terminal region of PrP without GdnHCl pretreatment, but usually very low
227 level. On the other hand, this band was not detected by antibodies recognizing the
228 N-terminal region of PrP (mAb 110 and 132, and pAb B103). These suggest that a
229 processing of region up to aa137 of the Chandler PrP^{Sc} occurs in the brain tissues albeit at
230 very low level. Alternatively, the processing may occur during the sample preparation or
231 autolysis.

232

233 **Conformational stability of PrP^{Sc} in cells infected with the Chandler strain.** Next,
234 we examined whether PrP^{Sc} in cells persistently infected with the Chandler strain shows the
235 region-dependent conformational stability. PrP^{Sc}-enriched fractions obtained from cell
236 lysates of ScN2a-5 were subjected to conformational-stability assays (Fig. 3). The mAb 110
237 detected the PK-resistant PrP^{Sc} bands with up to 1.5 M GdnHCl treatment, and the 1-2 kDa
238 smaller PrP^{Sc} bands were detected by pAb B103 with 2 and 2.5 M GdnHCl treatments.
239 Furthermore, the 6-7 kDa smaller N-terminally truncated PrP^{Sc} bands were detected by mAb
240 44B1 with even after 3 and 3.5 M GdnHCl treatment. These results were consistent with
241 those of PrP^{Sc} obtained from brains of mice infected with the Chandler strain, indicating that
242 the unique conformational stability was maintained in cultured cells.

243

244 **Conformational stability of the Chandler PrP^{Sc} in mice with different PrP genotypes.**

To examine whether the region-dependent conformational stability was maintained in mice with different genotypes, assays were carried out using brains of C57BL/6J (*Prnp*$^{a/a}$) and I/LnJ (*Prnp*$^{b/b}$) mice infected with the Chandler strain (Fig. 4). The patterns of PrP^{Sc} from C57BL/6J mice were almost identical to those from Jcl:ICR mice. In contrast to PrP^{Sc} from Jcl:ICR and C57BL/6J mice, the N-terminal region of PrP^{Sc} from I/LnJ mice was less resistant to GdnHCl; the $[GdnHCl]_{1/2}$ value of I/LnJ (1.2 M) was lower than those of Jcl:ICR and C57BL/6J mice (1.5 and 1.4 M, respectively) and PrP^{Sc} was undetected after the 1.5 M GdnHCl treatment by mAb 110. In addition, the C-terminus of PrP^{Sc} from I/LnJ mice appeared to be more stable than those from Jcl:ICR and C57BL/6J mice. Although a slight difference in the sensitivity to GdnHCl was observed, it should be emphasized that the sequential shift in molecular weight with an increase of GdnHCl concentration was reproduced in the Chandler PrP^{Sc} propagated in mice with *Prnp*$^{b/b}$ genotype; the 1-2 kDa smaller PrP^{Sc} bands were detected with pAB B103 at 1.5 and 2 M GdnHCl treatment, and the intensity of the 6-7 kDa smaller unglycosylated PrP^{Sc} detected with mAb 31C6 increased remarkably after 1.5 M or higher GdnHCl treatment. These results suggested that the region-dependent conformational stability of the PrP^{Sc} from the Chandler strain was maintained in mice with different PrP genotypes.

Effect of denaturation and removal of the N-terminal region of PrP^{Sc} on prion infectivity. To examine whether denaturation of specific regions of PrP^{Sc} affects the prion infectivity, brain homogenates from mice infected with the Chandler strain were treated with GdnHCl and subjected to bioassays. Small aliquots were analyzed by immunoblotting to confirm the region-specific denaturation of PrP^{Sc} in the inoculums (Fig. 5A). Survival times of mice inoculated with samples treated with 1 and 1.5 M GdnHCl were equivalent to those of the GdnHCl-untreated control (Table 2). Compared to the control (0 M, 159 ± 14 days),

survival time seemed to be prolonged by the 2 M GdnHCl treatment (176 ± 12 days); however, the difference was not statistically significant ($p > 0.05$). In contrast, significant prolongation was observed after the 3 M GdnHCl treatment (206 ± 25 days, $p < 0.01$). These results suggest that denaturation of the aa 81-137 of PrP^{Sc} greatly influences the prion infectivity. To confirm the involvement of the aa 81-137 in the prion infectivity more precisely, this region was removed by treatment with 3 M GdnHCl followed by PK digestion. The expected size shift of PrP^{Sc} in the inoculums was confirmed prior to the bioassay. Furthermore, the intensities of the PrP^{Sc} bands in samples treated with 0 and 3 M GdnHCl were relatively equivalent, indicating that an equal molar of PK-resistant PrP^{Sc} existed in the inoculums (Fig. 5B). These samples were intracerebrally inoculated into mice to examine the prion infectivity (Table 2). Compared to GdnHCl-untreated control (170 ± 11 days), sample treated with 3 M GdnHCl revealed an attack rate of 40% and a mean survival time of 235 days (n = 2). Furthermore, 2 out of 5 mice were still alive at 365 days post inoculation (dpi) (Table 2). These results suggest that the infectivity of the N-terminally truncated PK-resistant PrP^{Sc} lacking the aa 81-137 was extremely low.

In contrast to the Chandler strain, the immunoreactivity of PK-resistant PrP^{Sc} of the Obihiro strain decreased less than 1% of the original samples when the samples were treated with 3 M GdnHCl and following PK digestion (Fig. 5B). Consistent with the decrease of the amount of PrP^{Sc}, the survival time was prolonged for 34 days by treatment with 3 M GdnHCl (Table 2). From the dose-survival time standard curve for the Obihiro strain in ICR mice, the 34-day prolongation was estimated as more than a 2 Log reduction in infectivity.

DISCUSSION

Prion strains have been distinguished by their biological properties including incubation periods and neuropathological lesion profiles in mice experimentally inoculated with test samples (3, 4, 6, 7). However, these types of experiments are time-consuming and the results are difficult to standardize among laboratories. Biochemical properties of PrP^{Sc}, such as molecular weight, glycoforms, PK-resistance, and sensitivity to denaturants, often differ among prion strains (2, 5, 13, 25-27, 29), although relationship between the biochemical and biological properties are unclear. Elucidating the strain-specific biochemical properties as well as direct relationship between biochemical and biological properties will facilitate the distinction of prion strains without time-consuming bioassays and the understanding of the mechanisms involved in prion strains. From our analyses of the stability of PrP^{Sc} to the GdnHCl treatment with a panel of anti-PrP antibodies, we found that PrP^{Sc} of the Chandler strain possesses a unique region-dependent conformational stability. The aa 81-137 of PrP^{Sc} begins to be denatured by 1.5 M GdnHCl and is almost completely denatured and becomes PK-sensitive by 3 M GdnHCl treatment. By contrast, the C-terminal region (after aa 137) is extremely resistant to denaturation (Fig. 6).

When the blots in Fig. 2 were carefully examined, in the Chandler PrP^{Sc} treated with 2 and 2.5 M GdnHCl, the 1-2 kDa smaller di-glycosylated PrP^{Sc} was detected with mAbs 31C6 and 44B1, while the corresponding bands were unclear with mAbs 147 and 43C5. This suggests that the C-terminal region is also truncated in certain fraction of PrP^{Sc}. However, we think that the C-terminal truncation is not a major effect by the following reasons. First, affinity of mAbs and the amount of the 1-2 kDa smaller PrP^{Sc} influenced the result. The affinity of mAb 147 is lower than that of mAbs 31C6 and 44B1 (Sakata K. and Horiuchi M., in preparation), therefore, it is possible that mAb 147 could not visualize the relatively low amount of the 1-2 kDa smaller PrP^{Sc} in the samples treated with 2 and 2.5 M GdnHCl. Second, conformation of the particular region of PrP on the blot might influence the

interpretation of the results. The immunoreactivity of the 6-7 kDa smaller PrP^{Sc} increased when mAbs recognizing middle part of PrP were used (mAbs 31C6 and 43C5), especially, this tendency was obvious with mAb 43C5 (Fig. 2). We cannot explain the exact reason for this at the moment. However, the results suggest that the epitope of mAb 43C5 on the 6-7 kDa smaller PrP^{Sc} on the blot may be more easily-accessible than that on the regular and the 1-2 kDa smaller PrP^{Sc}. If these two types of molecules exist on the limited area of the blot, the reaction of mAb to the easily-accessible epitope will be pronounced. Although we do not exclude the possibility of the C-terminal truncation, further fine experiments will be required to address the C-terminal truncation.

The sequential size shift of PK-resistant PrP^{Sc} according to the denaturation was not observed in our study of other mouse-adapted prion strains, natural and experimental sheep scrapie and Japanese BSE cases (data not shown). Additionally, this property was maintained in mice with different *Prnp* genotypes and in cells persistently infected with the Chandler strain. Therefore, these results suggest that the region-dependent conformational stability is specific to PrP^{Sc} of the Chandler strain. In contrast, the conformational-stability assay of the RML prion, which is thought to be synonymous, or very close to the Chandler strain, showed no region-dependent conformational stability (19, 36). One possibility that explains this discrepancy is the use of different antibodies for PrP^{Sc} detection; Legname et al (19) and Thackray et al (36) used the Fab HuM-D18 that recognizes the aa 132-156 and mAb 683 that recognizes the aa 168-172, respectively. Both antibodies recognize the C-terminal region after the epitope for mAb 132, which should detect the molecular weight changes of PrP^{Sc} that possesses region-dependent conformational stability as found in Chandler strain. As these molecular weight changes were not detected in those studies, it is unlikely that the difference in antibodies accounts for the discrepancy. Alternatively, genetic backgrounds of mice used for prion propagation may cause the difference in the conformational stability. It

345 has been reported that the biochemical properties of PrP^{Sc} vary depending on the cell and
346 tissue types for prion propagation without changing biological properties (1). Indeed, mice
347 used for propagation of the RML prion in their study (CD-1 Swiss) were different from in this
348 study (Jcl:ICR and C57BL/6J). Thus, further analysis of the Chandler strain propagated in
349 various mice strains as well as analysis of other mouse-adapted prion strains, especially the
350 lineage of the Chandler strain such as 139A (6), will be required to conclude that the
351 region-dependent conformational stability is specific to the Chandler strain.
352 Legname et al (20) reported that a linear correlation between the $[GdnHCl]_{1/2}$ values and
353 incubation periods. In contrast, no linear correlation was observed in our results ($n = 9$, $r =$
354 13, $\gamma^2 = 0.019$). We think that sample size in our study too small to make any conclusion.
355 Especially, few data are available for strains showing longer incubation periods or higher
356 $[GdnHCl]_{1/2}$ values at present. Therefore, further accumulation of data will be required to
357 assess the correlation between incubation periods and conformational stabilities of PrP^{Sc}.
358 PrP^{Sc} is comprised of PK-sensitive and PK-resistant PrP^{Sc} (2, 29, 30, 37). Both types of
359 PrP^{Sc} are infectious and PK digestion alone decreases prion infectivity to some extent (2, 31).
360 However, it is well known that the PK-resistant core of PrP^{Sc}, called as PrP27-30, which is
361 produced by the removal of PK-sensitive N-terminal region of PrP^{Sc} (from aa 23 to around
362 90), possesses prion infectivity. Prions propagated in Tg mice expressing PrP that lacks the
363 aa 23-88 can propagate in mice expressing wild-type PrP (18). These previous results
364 indicate that this N-terminal region of PrP^{Sc} is not essential for the infectivity of prion.
365 However, analyzing the relationship between other regions of PrP^{Sc} and infectivity by making
366 deletions or mutations has been difficult. In this study, we utilized the region-dependent
367 conformational stability of the Chandler PrP^{Sc} and truncated the PrP^{Sc} directly at the
368 N-terminal region up to around aa 137 to produce the N-terminally truncated PK-resistant
369 PrP^{Sc}; this allowed us to then analyze the influence of this region on prion infectivity.

370 Compared to the regular PK-resistant core of PrP^{Sc} that is produced by PK digestion without
371 GdnHCl treatment, the infectivity of the N-terminally truncated PK-resistant PrP^{Sc} was
372 extremely low despite the C-terminal region existed as PK-resistant fragments (Table 2).
373 Since we have not had a dose-incubation standard curve for the Chandler strain in Jcl:ICR
374 mice, we cannot estimate the exact reduction rate. However, the attack rate and the survival
375 time suggested that the infectivity decreased to nearly the detection limit in the bioassay.
376 This provides direct evidence that the aa 81-137 of PK-resistant PrP^{Sc} is critical for prion
377 infectivity, although evidence for other prion strains remains to be elucidated. However,
378 PK-treatment alone reduced the infectivity of the Chandler strain (159 and 170 days without
379 and with PK-treatment, respectively, in Table 2), indicating that there is the PK-sensitive PrP^{Sc}
380 fraction possessing prion infectivity in the brain homogenates of the Chandler strain-infected
381 mice. Our results clearly showed that the aa 81-137 of the PK-resistant core of the Chandler
382 PrP^{Sc} is important for the infectivity, however, it remains unclear whether the same is
383 applicable to the infectivity of the PK-sensitive PrP^{Sc} fraction.
384 Compared to the removal of this region, the denaturation of this region by 3 M GdnHCl
385 treatment appeared less effective in reducing prion infectivity. However, considering the
386 effect of GdnHCl on PrP^{Sc} aggregates, the denaturation itself appears to result in a substantial
387 loss of infectivity (Table 2). The GdnHCl treatment has two expected effects; dissociation of
388 large PrP^{Sc} aggregates into small aggregates and denaturation of the PrP^{Sc} molecules. Hence,
389 without PK digestion, small aggregates consisting of PrP^{Sc} with incompeletely denatured aa
390 81-137 may remain and infectivity may be observed. Such small PrP^{Sc} aggregates should be
391 PK-sensitive and therefore the infectivity should be diminished after PK digestion (31).
392 Alternatively, this region may have been somewhat refolded after the GdnHCl treatment,
393 which would lead to infectivity.
394 Several distinct domains of PrP^{C} are reported to be involved in the direct interaction to